

Strong Effects of Cation Vacancies on the Electronic and Dynamical Properties of FeO

Urszula D. Wdowik,¹ Przemysław Piekarz,² Krzysztof Parlinski,² Andrzej M. Oleś,^{3,4} and Józef Korecki^{5,6}

¹*Institute of Technology, Pedagogical University, Podchorążych 2, PL-30084 Kraków, Poland*

²*Institute of Nuclear Physics, Polish Academy of Sciences, Radzikowskiego 152, PL-31342 Kraków, Poland*

³*Marian Smoluchowski Institute of Physics, Jagellonian University, Reymonta 4, PL-30059 Kraków, Poland*

⁴*Max-Planck-Institut für Festkörperforschung, Heisenbergstrasse 1, D-70569 Stuttgart, Germany*

⁵*Jerzy Haber Institute of Catalysis and Surface Chemistry, Polish Academy of Sciences, Niezapominajek 8, PL-30239 Kraków, Poland*

⁶*Faculty of Physics and Applied Computer Science, AGH University of Science and Technology, aleja Mickiewicza 30, PL-30059 Kraków, Poland*

(Dated: June 19, 2021)

We report pronounced modifications of electronic and vibrational properties induced in FeO by cation vacancies, obtained within density functional theory incorporating strong local Coulomb interactions at Fe atoms. The insulating gap of FeO is reduced by about 50% due to unoccupied electronic bands introduced by trivalent Fe ions stabilized by cation vacancies. The changes in the electronic structure along with atomic displacements induced by cation vacancies affect strongly phonon dispersions via modified force constants, including those at atoms beyond nearest neighbors of defects. We demonstrate that theoretical phonon dispersions and their densities of states reproduce the results of inelastic neutron and nuclear resonant x-ray scattering experiments *only* when Fe vacancies and Coulomb interaction U are both included explicitly in *ab initio* simulations, which also suggests that the electron-phonon coupling in FeO is strong.

PACS numbers: 71.30.+h, 63.20.dk, 63.20.kp, 71.23.An

As explained by the theory of Mott¹ and Hubbard,² the insulating state in transition metal oxides results from the electron localization in the narrow $3d$ band due to the local Coulomb interactions.³ Iron oxides are in the focus of present-day research covering a broad range of complex phenomena such as the Verwey transition in magnetite⁴ or structural instabilities in polar nanosystems.⁵ High-resolution neutron and x-ray scattering experiments on magnetite⁶ suggest a considerably more complex charge order than originally invoked by Verwey.⁷ It has been shown that the microscopic understanding of this phenomenon requires full information about both the electronic structure and the lattice dynamics in the presence of strong electron interactions which significantly amplify the electron-phonon coupling, as predicted in the theory⁸ and confirmed recently by inelastic x-ray scattering.⁹ This could be a common feature of iron oxides — indeed, the exchange-induced phonon splitting observed in wüstite¹⁰ suggests a strong coupling between electronic and lattice degrees of freedom.

Wüstite, Fe_{1-x}O , is another strongly correlated insulator within iron oxides, with the insulating energy gap of ~ 2.4 eV arising mainly from the $\text{O}(2p) \rightarrow \text{Fe}(3d)$ charge-transfer process.¹¹ Below the Néel temperature $T_N = 198$ K antiferromagnetic (AF) order sets in, which suggests that also here strong on-site Coulomb interaction U plays a role. A stable crystal of Fe_{1-x}O shows large Fe-deficiency on the level $0.05 < x < 0.15$,¹² which substantially influences its structural properties.^{13,14} It may also affect the geophysical processes in the Earth's lower mantle where wüstite, existing in the (Mg,Fe)O solid solution, is one of the most important constituents.¹⁵ So far, first-principles investigations on a vacancy-defected FeO¹⁶

and other transition metal oxides^{17,18} are scarce. Previous studies were devoted to the stoichiometric FeO,^{19,20} leaving the effect of cation vacancies on the electronic and lattice properties of wüstite largely unexplored.

At room temperature, Fe_{1-x}O crystallizes in a rock-salt structure and exhibits the rhombohedral distortion with a weak elongation along the [111] direction in the AF phase below T_N . The magnetic moments on the Fe cations are aligned perpendicular to the ferromagnetically ordered (111) planes reversing their orientations from one to another plane.²¹ Due to the cation deficiency and crystal-field effects, the average magnetic moment $m = 3.32\mu_B$ measured at 4.2 K is significantly reduced from the ionic Fe^{2+} value $m = 4\mu_B$ (for spin $S = 2$).²² Large splitting of phonon modes below T_N indicates strong spin-phonon coupling in wüstite.¹⁰

In this Rapid Communication we demonstrate that Fe vacancies (V_{Fe}) strongly modify the structural, electronic, and vibrational properties of wüstite. Our theoretical investigations uncover qualitative difference between stoichiometric FeO and defected Fe_{1-x}O containing either 3% or 6% of cation vacancies. The present *ab initio* results for Fe_{1-x}O are in good agreement with the available experimental data from inelastic neutron scattering (INS)²³ and nuclear resonant inelastic x-ray scattering (NRIXS),²⁴ which validates our findings.

Notably, a realistic description of the electronic structure of Mott insulating states in transition metal monoxides requires methods which implement explicitly local Coulomb interactions.^{25,26} Previous theoretical studies within the local density approximation (LDA) using the Coulomb interaction U (LDA+ U)^{27,28} confirmed the prominent role of local electron interactions on the band

structure of defect-free FeO and significant contribution of the O($2p$) states at energies just below the Fermi energy. Cation vacancies are responsible for charge redistribution and appearance of trivalent Fe ions in the octahedral and tetrahedral (interstitial) positions.^{14,16} The highly correlated nature of $3d$ electronic states has also a strong impact on the lattice dynamics of transition metal oxides. The experimental data have been well reproduced within the LDA+ U approach²⁸ applied to NiO,²⁹ CoO,³⁰ and MnO;³¹ further improvements were obtained in the Green's function approach.³² Until now, lattice dynamics of stoichiometric FeO has only been studied in a semiempirical model.³³

The present calculations were performed within the generalized gradient approximation (GGA) and the projector augmented-wave method³⁴ implemented in the VASP code.³⁵ The on-site interactions at Fe ions are: the Coulomb element $U = 6$ eV and Hund's exchange $J = 1$ eV.^{20,27} The AF supercell composed of 64 atoms was used to calculate stoichiometric FeO. The Fe_{1-x}O crystals with $x = 3\%$ and $x = 6\%$ were modeled by removing either one or two Fe atoms from the optimized AF supercell. Various $V_{\text{Fe}}-V_{\text{Fe}}$ distances within the simulated supercell with $x = 6\%$ were considered. Finally, a configuration with the lowest energy, corresponding to the distance between two vacancies of $1.22a$, with a being the lattice constant of the perfect FeO, was chosen for further band structure and phonon calculations. The energy difference between the lowest and the next stable configuration amounts to 7 meV/atom indicating rather high mobility (diffusion) of vacancies in wüstite. The volumes of the supercells representing Fe_{1-x}O systems were fixed at the optimized value of the vacancy-free lattice, the symmetry constraints were removed, and all atoms were allowed to relax.

We identified two distinct valence states of Fe cations for each Fe_{1-x}O composition. Majority of cations are Fe^{2+} ions with moments $m = 3.72\mu_B$, but there are two iron ions per each V_{Fe} that have enhanced charges and moments ($m = 4.22\mu_B$). For single-vacancy system, they are located at distances a and $1.73a$ from V_{Fe} . The Bader charge analysis³⁶ indicates an increase in their valence charges by $+0.31e$ over the valence of Fe^{2+} ions. We assign the above features to the Fe^{3+} ions.

The orbital projected electron densities of states (DOS) for FeO and the two Fe_{1-x}O systems considered here are dominated by the O($2p$) and Fe($3d$) states; the latter showing the crystal-field splitting between the t_{2g} and e_g symmetry. As in the previous studies,¹⁹ the electronic states close to the energy gap are occupied by the minority spin t_{2g} electrons, see Fig. 1. The empty Fe($3d$) states are split and shifted to higher energies due to the Hubbard interaction U , while the O($2p$) states are almost fully occupied and hybridize with the Fe($3d$) states in a broad energy range below the Fermi energy.

We observe significant modifications of the electronic structure for the system with incorporated cation vacancies. First of all, the projected electronic DOS becomes

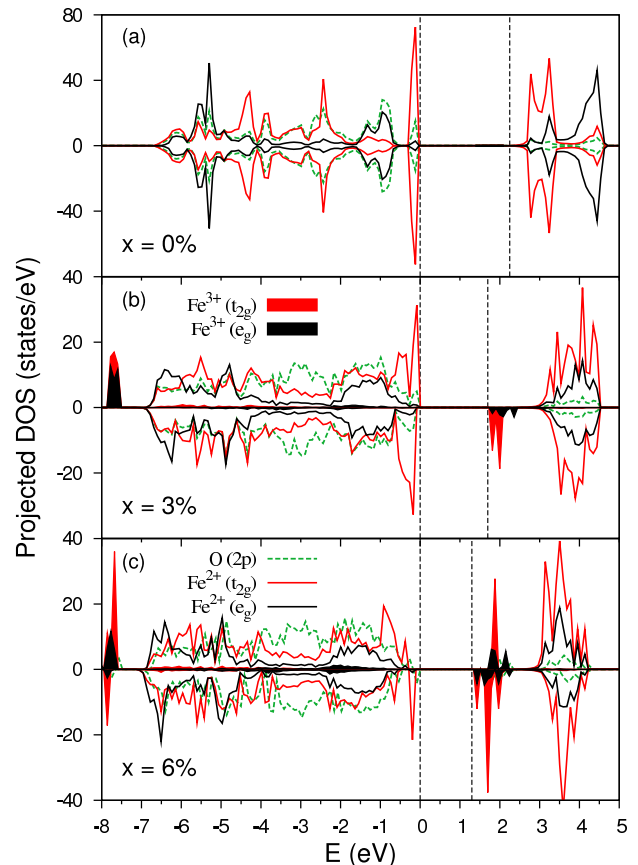


FIG. 1. (Color online) Total orbital projected electronic DOS obtained for: (a) the stoichiometric FeO, and defected Fe_{1-x}O , with (b) $x = 3\%$, and (c) $x = 6\%$. The positive (negative) DOS represents the spin-up (spin-down) states in each case; the gaps between the valence and conduction band are indicated by dashed lines. Parameters: $U = 6$ eV, $J = 1$ eV.

asymmetric in the distribution of the spin-up and spin-down components of the $3d$ states after removing one Fe cation from the spin-down sublattice. Also, unlike in the stoichiometric FeO, see Fig. 1(a), the oxygen bands of the wüstite crystals with different concentration of Fe vacancies remain spin-polarized. Each V_{Fe} induces changes in the charge distribution of its immediate neighborhood, pushing the O($2p$) states closer to the Fermi energy. As the most interesting feature we identify additional electronic bands that originate from the $3d$ states of Fe^{3+} ions. In Fe_{1-x}O with $x = 3\%$, the occupied $3d$ states of Fe^{3+} ions form a narrow band at about -7.6 eV, see Fig. 1(b). It lies below the main manifold of the Fe^{2+} states and consists of all five Fe($3d$) states. The unoccupied Fe^{3+} ($3d$) states appear as the lowest energy empty states and reduce the insulating energy gap of wüstite from ~ 2.2 eV to ~ 1.8 eV.³⁷ Spin polarization of the Fe^{3+} states depends on the Fe (spin-up or spin-down) sublattice into which the V_{Fe} is introduced. The electronic bands due to the trivalent Fe ions in the Fe_{1-x}O system with $x = 6\%$ exist in both spin channels as the

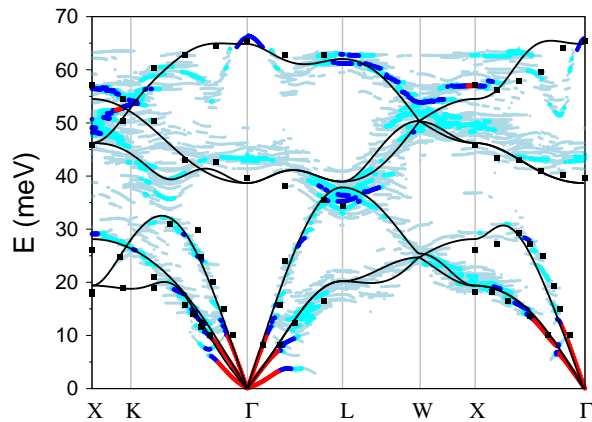


FIG. 2. (Color online) Phonon dispersion relations for stoichiometric FeO (solid lines) and the relative intensities of the phonon modes in Fe_{1-x}O with $x = 3\%$, for $U = 6$ eV, $J = 1$ eV. The experimental data (solid squares) are adopted from Ref.²³. The highest intensity mode is taken as a reference (100%); relative intensities are arranged into the following ranges indicated by the intensity of gray scale (color): 5-20% (\square), 20-50% (\square), 50-80% (\square), 80-100% (\square). High-symmetry points are (in units of $2\pi/a$): $\Gamma = (0, 0, 0)$, $X = (\frac{1}{2}, \frac{1}{2}, 0)$, $K = (\frac{3}{8}, \frac{3}{8}, \frac{3}{4})$, $L = (\frac{1}{2}, \frac{1}{2}, \frac{1}{2})$, $W = (\frac{1}{2}, \frac{1}{4}, \frac{3}{4})$.

cation vacancies occupy both spin-sublattices. A larger concentration of vacancies $x = 6\%$ broadens electronic bands and leads to further decrease of the insulating gap to the value of ~ 1.3 eV³⁸. This value is quite close to the observed optical gap of ~ 1.0 eV.¹⁰ The electronic states induced by disorder are expected to influence transport properties of FeO.³⁹

Phonons in FeO and Fe_{1-x}O were determined by the direct method,⁴⁰ where the Hellmann-Feynman forces were obtained by displacing all symmetry non-equivalent atoms from their equilibrium positions with the amplitude of 0.03 Å and applying both positive and negative displacements to minimize systematic error.³⁵ The transverse optic (TO) phonon modes followed directly from the diagonalization of the dynamical matrix,⁴⁰ while the longitudinal optic (LO) modes were obtained by introducing into the dynamical matrix the non-analytical term,⁴¹ the latter dependent on the Born effective charge tensor \mathbf{Z}^* and the electronic part of dielectric constant ϵ_∞ . Both \mathbf{Z}^* and ϵ_∞ were determined within the linear response method⁴² implemented in the VASP code. Our calculations resulted in $|Z_{\text{Fe}}^*| = |Z_{\text{O}}^*| = 2.2$ and $\epsilon_\infty = 5.262$.⁴³ ϵ_∞ and $|Z^*|$ averaged over particular sublattices remain almost insensitive to the incorporated cation vacancies,⁴⁴ whereas the Fe³⁺ ions acquire the effective dynamical charge of +1.3 over that for Fe²⁺ ions.

Imposed cubic symmetry constraints result in 6 phonon branches. The transverse acoustic (TA) and TO phonon modes remain doubly degenerate along the Γ - X and Γ - L directions. Despite an apparent correlation between our theoretical curves and the INS data,⁴⁵ we notice some discrepancies for the TO branch close to the

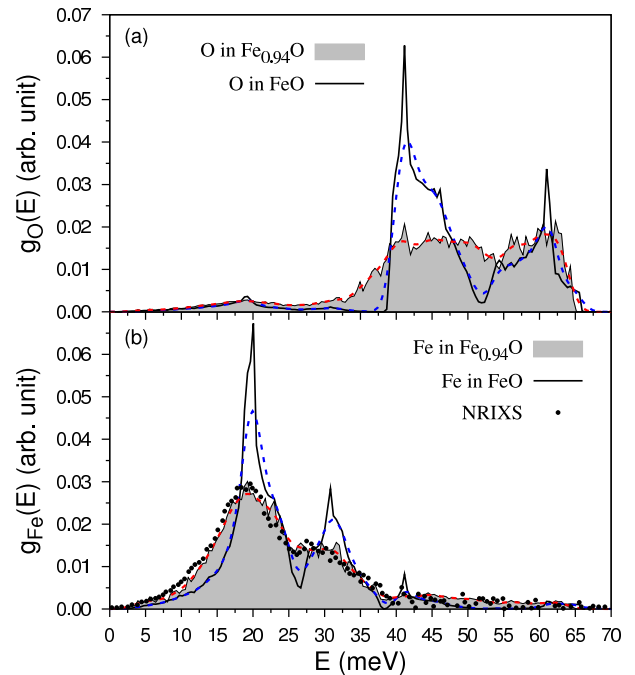


FIG. 3. (Color online) Partial phonon DOS obtained for stoichiometric FeO (solid lines) and Fe_{1-x}O with $x = 6\%$ (shaded area) for sublattice of: (a) oxygen and (b) iron ions. Experimental points in (b) are taken from the NRIXS experiment.²⁴ Dotted lines denote the Gaussian convolutions of our theoretical results with the experimental resolution of 2.4 meV. Parameters: $U = 6$ eV, $J = 1$ eV.

L point and the longitudinal acoustic (LA) branch near the X point, see Fig. 2. An evident departure of the calculated LO branch from the experimental points along the $\Gamma - X$ direction is mainly due to the interpolation function used here to calculate the LO-TO splitting.⁴⁰

Some of the above discrepancies can be explained by considering phonons in the FeO crystals defected by cation vacancies. However, we have to remark that an elaboration of the resulting phonon dispersion curves in the system with point defects requires a special treatment which involves application of the phonon form factor.⁴⁶ We follow the same methodology as used before for the strongly correlated CoO with various point defects (cation vacancies and Fe impurities).¹⁸ The resulting intensities of the phonon modes in Fe_{1-x}O with $x = 3\%$ are overlaid onto the phonon dispersions for the stoichiometric FeO in Fig. 2. Discontinuities in some phonon branches come from the 5% cut-off applied to the relative intensities of the phonon modes in Fe_{1-x}O. Although the calculated phonon spectrum is dominated by the modes of low relative intensities, the INS data concentrate close to the modes with intensities exceeding 30%. Moreover, the calculated phonons at the Brillouin zone boundaries, e.g. at the L and X points, match better the experimental data. Finally, despite many similarities between the phonon spectra of FeO with 3% and 6% vacancies, the system with doubled vacancy concentration exhibits

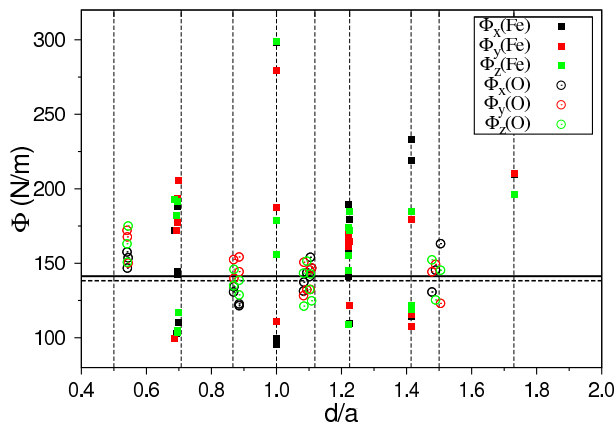


FIG. 4. (Color online) Diagonal elements Φ of the on-site force-constants matrix for distance d/a from the vacancy in the Fe_{1-x}O system with $x = 3\%$. Vertical dashed lines denote ideal positions of the Fe and O atoms, whereas the horizontal solid and dashed lines stand for the respective force constants in the stoichiometric FeO. Parameters: $U = 6$ eV, $J = 1$ eV.

significantly more phonon modes carrying low intensities.

Essential differences in the dynamics of the stoichiometric and defected lattices are revealed by the phonon DOS, see Fig. 3. Here, our theoretical results of partial Fe DOS obtained for stoichiometric FeO and Fe_{1-x}O with $x = 6\%$ are compared to the experimental data of NRIXS²⁴ performed on the wüstite sample with the non-stoichiometry of 5.3%, see Fig. 3(b). The iron and oxygen contributions span different energy ranges which overlap weakly due to large difference between their masses. Both convoluted and bare theoretical phonon spectra of stoichiometric FeO show quite narrow and well-resolved peaks, opposite to the broad phonon maxima in the Fe_{1-x}O spectra. These latter spectra agree remarkably well with the experimental results.²⁴ A smearing of the two-peak structure, inevitably connected with the presence of Fe vacancies, becomes even more enhanced for the O-sublattice, indicating its greater sensitivity to the changes in the local crystal environment.

To clarify the origin of changes in atomic vibrations, we have analyzed the force constant matrix for the wüstite crystal with $x = 3\%$, see Fig. 4. The on-site force constants Φ_α along the main crystallographic axes $\alpha = x, y, z$ increase for the vacancy neighboring oxygen atoms over

the respective ones in the idealized vacancy-free FeO. They are displaced outward the vacancy by ~ 0.18 Å. On the other hand, the O atoms occupying the subsequent shells are attracted toward the nearest Fe atoms and their force constants remain equally distributed around the value corresponding to the perfect lattice. Similar but weaker effects on force constants have also been encountered in the cation-deficient CoO.¹⁸

Relaxations of the atomic positions in the Fe-sublattice are less pronounced, except the second nearest neighbors to a vacancy which shift closer to it.⁴⁷ The force constants at the iron sites show considerably broader distribution range than those at oxygens sites. Moreover, the force constants at Fe^{3+} ions are significantly enhanced from their values at Fe^{2+} ions, with the largest values of Φ_α at the distance a from V_{Fe} . This clearly demonstrates a strong impact of the wüstite electronic structure on its interatomic forces and accounts for the observed broadening of peaks in the phonon DOS. It may also explain large spectral linewidths of the dielectric loss function and strong electron-phonon coupling observed recently for FeO with the nonstoichiometry of 7-8%.¹⁰ Such pronounced changes in the phonon DOS, in particular the excess of spectral intensity at lowest energies, influence also thermodynamic properties of FeO. For instance, in case of one cation vacancy the calculations predict the increase of lattice heat capacity at $T = 50$ K by about 10% over the stoichiometric FeO, and enhanced thermal atomic displacements in the neighborhood of a vacancy.

Summarizing, we have reported dramatic changes of the electronic structure and vibrational spectra of wüstite caused by cation vacancies. Significant charge redistribution on Fe ions induces the empty electronic states above the valence band and strongly reduces the insulating gap. The changes in the electronic structure and atomic displacements generated by defects substantially modify the force constants not only in the immediate neighborhood of vacancies but also at more distant atoms. It results in broadening of peaks in the phonon spectra, in close agreement with available experimental data. Predicted changes in the dynamics of the oxygen sublattice in Fe_{1-x}O provide an experimental challenge that could be resolved, for example, by incoherent INS experiments.

Acknowledgments. — P. Piekarz and A.M. Oleś kindly acknowledge financial support by the Polish National Science Center (NCN) under Projects No. 2011/01/M/ST3/00738 and No. 2012/04/A/ST3/00331.

¹ N. F. Mott, Proc. Phys. Soc. A **62**, 416 (1949).

² J. Hubbard, Proc. R. Soc. London A **277**, 237 (1964).

³ M. Imada, A. Fujimori, and Y. Tokura, Rev. Mod. Phys. **70**, 1039 (1998).

⁴ F. Walz, J. Phys. Condens. Matter **14**, R285 (2002).

⁵ J. Goniakowski, F. Finocchi, and C. Noguera, Rep. Prog. Phys. **71**, 016501 (2008).

⁶ J. P. Wright, J. P. Attfield, and P. G. Radaelli, Phys. Rev.

Lett. **87**, 266401 (2001); Phys. Rev. B **66**, 214422 (2002).

⁷ E.J.W. Verwey, Nature (London) **144**, 327 (1939).

⁸ P. Piekarz, K. Parlinski, and A. M. Oleś, Phys. Rev. Lett. **97**, 156402 (2006); Phys. Rev. B **76**, 165124 (2007).

⁹ M. Hoesch, P. Piekarz, A. Bosak, M. Le Tacon, M. Krisch, A. Kozłowski, A. M. Oleś, and K. Parlinski, arXiv:1303.2888 (unpublished).

¹⁰ Ch. Kant, M. Schmidt, Zhe Wang, F. Mayr, V. Tsurkan,

- J. Deisenhofer, and A. Loidl, Phys. Rev. Lett. **108**, 177203 (2012); F. Schrettle, Ch. Kant, P. Lunkenheimer, F. Mayr, J. Deisenhofer, and A. Loidl, Eur. Phys. J. B **85**, 164 (2012).
- ¹¹ J. Zaanen, G. A. Sawatzky, and J. W. Allen, Phys. Rev. Lett. **55**, 418 (1985); A. Fujimori, N. Kimizuka, M. Taniguchi, and S. Suga, Phys. Rev. B **36**, 6691 (1987).
- ¹² Among the simple $3d$ transition metal oxides, NiO and FeO display respectively much lower and much higher deviations from stoichiometry, while MnO and CoO show behavior intermediate to these two extremes.
- ¹³ W. L. Roth, Acta Crystallogr. **13**, 40 (1960); F. Koch and J. B. Cohen, Acta Crystallogr. B **25**, 275 (1969).
- ¹⁴ A. K. Cheetham, B. E. F. Fender, and R. I. Taylor, J. Phys. C.: Solid State Phys. **4**, 2160 (1971); C. R. A. Catlow and B. E. F. Fender, *ibid.* **8**, 3267 (1975).
- ¹⁵ A. E. Ringwood, Geochim. J. **11**, 111 (1977).
- ¹⁶ M. R. Press and D. E. Ellis, Phys. Rev. B **35**, 4438 (1987); P. K. Khowash and D. E. Ellis, *ibid.* **39**, 1908 (1989).
- ¹⁷ D. Ködderitzsch, W. Hergert, Z. Szotek, and W. M. Temmerman, Phys. Rev. B **68** 125114 (2003); S. Park, H.-S. Ahn, C.-K. Lee, H. Kim, H. Jin, H.-S. Lee, S. Seo, J. Yu, and S. Han, *ibid.* **77**, 134103 (2008).
- ¹⁸ U. D. Wdowik and K. Parlinski, Phys. Rev. B **78**, 224114 (2008); J. Phys. Condens. Matter **21**, 125601 (2009).
- ¹⁹ V. I. Anisimov, M. A. Korotin, and E. Z. Kurmaev, J. Phys. Condens. Matter **2**, 3973 (1990); A. O. Shorikov, Z. V. Pchelkina, V. I. Anisimov, S. L. Skornyakov, and M. A. Korotin, Phys. Rev. B **82**, 195101 (2010).
- ²⁰ F. Tran, P. Blaha, K. Schwarz, and P. Novák, Phys. Rev. B **74**, 155108 (2006).
- ²¹ C. G. Shull, W. A. Strauser, and E.O. Wollan, Phys. Rev. **83**, 333 (1951).
- ²² W. L. Roth, Phys. Rev. **110**, 1333 (1958).
- ²³ G. Kugel, C. Carabatos, B. Hennion, B. Prevet, A. Revcolevschi, and D. Tocchetti, Phys. Rev. B **16**, 378 (1977).
- ²⁴ V. V. Struzhkin, H.-K. Mao, J. Hu, M. Schwoerer-Böhning, J. Shu, R. J. Hemley, W. Sturhahn, M. Y. Hu, E. E. Alp, P. Eng, and G. Shen, Phys. Rev. Lett. **87**, 255501 (2001).
- ²⁵ I. V. Solovyev, J. Phys. Condens. Matter **20**, 293201 (2008); R. Eder, Phys. Rev. B **78**, 115111 (2008).
- ²⁶ M. Imada and T. Miyake, J. Phys. Soc. Jpn. **79**, 112001 (2010).
- ²⁷ V. I. Anisimov, J. Zaanen, and O. K. Andersen, Phys. Rev. B **44**, 943 (1991).
- ²⁸ A. I. Liechtenstein, V. I. Anisimov, and J. Zaanen, Phys. Rev. B **52**, R5467 (1995); V. I. Anisimov, F. Aryasetiawan, and A. I. Liechtenstein, J. Phys.: Condens. Matter **9**, 767 (1997).
- ²⁹ S. Y. Savrasov and G. Kotliar, Phys. Rev. Lett. **90**, 056401 (2003).
- ³⁰ U. D. Wdowik and K. Parlinski, Phys. Rev. B **75**, 104306 (2007); **77**, 115110 (2008); U. D. Wdowik, Phys. Rev. B **84**, 064111 (2011).
- ³¹ U. D. Wdowik and D. Legut, J. Phys. Condens. Matter **21**, 275402 (2009).
- ³² S. Massidda, M. Posternak, A. Baldareschi, and R. Resta, Phys. Rev. Lett. **82**, 430 (1999).
- ³³ K. S. Upadhyaya, G. K. Upadhyaya, and M. Yadav, J. Phys. Soc. Jpn. **70**, 723 (2001).
- ³⁴ P. E. Blöchl, Phys. Rev. B **50**, 17953 (1994); G. Kresse and D. Joubert, *ibid.* **59**, 1758 (1999).
- ³⁵ G. Kresse and J. Furthmüller, Comput. Mater. Sci. **6**, 15 (1996).
- ³⁶ R. Bader, *Atoms in Molecules: A Quantum Theory* (Oxford University Press, New York, 1990); G. Henkelman, A. Arnaldsson, and H. Jónsson, Comput. Mater. Sci. **36**, 254 (2006).
- ³⁷ The electronic states are localized inside the insulating gap also in the vacancy-defected CoO,³⁰ in stark contrast to MnO and NiO where cation vacancies induce only shallow states.¹⁷
- ³⁸ Estimates imply that the Mott-Hubbard gap closes at $U < 4$ eV for each composition.
- ³⁹ The coupling between electrons and lattice distortions in defected structure may be responsible for polaronic character of charge carriers observed at low temperatures.¹⁰
- ⁴⁰ K. Parlinski, Z. Q. Li, and Y. Kawazoe, Phys. Rev. Lett. **78**, 4063 (1997); K. Parlinski, software PHONON (Cracow, Poland, 2011).
- ⁴¹ R. M. Pick, M. H. Cohen, and R. M. Martin, Phys. Rev. B **1**, 910 (1970).
- ⁴² M. Gajdos, K. Hummer, G. Kresse, J. Furthmüller, and F. Bechstedt, Phys. Rev. B **73**, 045112 (2006).
- ⁴³ The small rhombohedral distortions of the stoichiometric FeO lattice were neglected and under such an assumption both Z^* and ϵ_∞ tensors could be described by single parameters $|Z^*|$ and ϵ_∞ , respectively.
- ⁴⁴ $\epsilon_\infty = 5.261$ and $\epsilon_\infty = 5.483$ were obtained for the Fe_{1-x}O systems with $x = 3\%$ and $x = 6\%$, respectively. Averaged $|Z_{\text{Fe}}^*| = 2.3$ and $|Z_{\text{Fe}}^*| = 2.4$ are found for Fe ions in the systems with $x = 3\%$ and $x = 6\%$, respectively. No changes were observed for average O charge $|Z_{\text{O}}^*|$.
- ⁴⁵ Such a good agreement between the experimental data and the calculated phonon dispersions could be obtained only with $U \simeq 6$ eV and $J \simeq 1$ eV; at $U = J = 0$ one finds much poorer agreement including soft mode behavior.
- ⁴⁶ A. Sjölander, Ark. Fys. **14**, 315 (1958).
- ⁴⁷ Such displacement pattern results from the attraction between the vacancy and Fe cations and is consistent with the diffuse neutron scattering data, see: W. Schweika, A. Hoser, M. Martin, and A. E. Carlsson, Phys. Rev. B **51**, 15771 (1995).